A modelling approach to uncovering host-specific interactions by jumbo phage FLC4-4c

Written by: Leroy van der Meer
Daily supervisor: Shuhei MIYASHITA
Examiners: Shuhei MIYASHITA & Rob de Boer
Tohoku University, Plant Pathology
26-07-2024

Layman's summary

Growing crops in a field comes with many challenges. Like with humans, the presence of bacteria can cause disease and make growth more difficult or impossible. The use of chemicals is an effective and common way of reducing bacterial concentrations in the field. Unfortunately, the side effects of using such chemicals on the health of the environment and consumers have prompted a search for alternatives. Fortunately, just like humans and plants, bacteria are not exempt from disease threats. Viruses specifically infecting bacteria, also known as bacteriophages, have been identified. Moreover, Jumbo phages, which are particularly large genomes and are capable of infection a variety of bacteria have been proposed as attractive alternatives to chemical treatments. In this project, we use computer simulations to predict the interactions between these Jumbo phages and bacteria.

Abstract

The predicted increase in global temperature is expected to raise bacterial infections in rice (Oryza sativa). A common cause of crop yield loss in rice is *Burkholderia glumae*, which causes rice seedling rot among other diseases. Recent efforts in developing bacteriophage-based treatments for *B. glumae* infection have identified a Jumbo phage FLC4-4c as a potential candidate. This Jumbo phage has a wide host range and is capable of infecting both *Burkholderia plantarii* and *Burkholderia gladioli.* However, while performing plaque assays on *B. plantarii* bacterial lawns, the phage suddenly loses its ability to infect. In this project, we validate the experimentally found abrupt disappearance in plaque formation. Besides that, we set up a cellular automaton to simulate the spread and infection of bacteria on plates. Dispite the implementation of alternative density-dependent resistance mechanisms in the bacteria, we were unable to recreate the abrupt disappearance as observed previously. Regardless, our base model can simulate the spread of infection and our parameters show the jumbo phage has a uniquely large burst size of 200 while retaining an average latent period of 180 min.

Keywords: Jumbo phage*, Burkholderia plantarii, Ralstonia pseudosolanacearum,* Cellular automaton, Plaque assay.

Introduction

Over the last five years, the combined annual rice production of the top 10 rice-producing countries was 520 million tons, according to the USDA ERS. A major disease in rice production is 'bacterial grain rot' or 'bacterial panicle blight', which can cause a yield loss of up to 75% in severe cases (HAM et al., 2010). This disease is mainly caused by *Burkholderia glumae* and can affect the seedlings, sheath, and grains of the rice (HAM et al., 2010). Other closely related bacteria, such as *Burkholderia plantarii* (Adachi et al., 2012) and *Burkholderia gladioli* (HAM et al., 2010) have also been isolated from rice plants with bacterial grain rot infections.

In recent years, two *Burkholderia* Jumbo phages, FLC6 & FLC4-4c, were isolated from leaf-litter material (Sasaki et al., 2021). FLC6 has been shown to infect a wide range of hosts, including *B. glumae* and *B. plantarii* (Sasaki et al., 2021). Jumbo phages, which have genomes larger than 200 kbp, have been proposed as biocontrol agents

in the past (Kanaizuka et al., 2023). Due to their increased genome size, jumbo phages have a wider host range compared to regular phages (Kanaizuka et al., 2023).

Infection of host bacteria by phages is studied using plaque assays (Adachi et al., 2012). Here a layer of growth media mixed with bacterial cells is treated with phages. The successful infection and lysis of bacteria result in clear spots (plaques) in the otherwise opaque media (Abedon & Culler, 2007a). Generally, these plaques are assumed to form from single phage particles that elicited successful infections. The size of a single plaque is limited, while the morphology of the edge can vary (Gallet et al., 2011). The number of plaques can be used to calculate the phage concentration in the phage solution.

Preliminary data has shown an interesting pattern when treating *B. plantarii* with FLC4-4c: instead of a gradual decline in PFUs throughout the dilution series, there is an abrupt disappearance. This phenomenon persists even after repeating the experiment. In contrast, the commonly used *Ralstonia pseudosolanacearum* and *B. glumae* show the expected gradual decrease in PFUs.

In this project, we investigate the abrupt disappearance of PFUs in some bacterial hosts via the use of computational models. By utilising a cellular automaton to simulate bacterial proliferation on a plate and adding a phage layer that spreads based on host availability, we aim to explore the factors contributing to this phenomenon. Phage characteristics such as burst size, burst time, and diffusion rate have been proposed as prime determinants of plaque size (Gallet et al., 2011). Therefore, characterizing these factors in wet lab experiments will be crucial for creating the model. Previous work proposed nutrient availability as a driving factor in FLC4-4c proliferation (Miyashita Unpublished). Here, we test this along with density-dependent resistance, and sacrificial behaviour.

Additionally, a model of bacterial and phage propagation in liquid culture will be developed. This is relevant to the plaque assay conditions as well as phage propagation for other experiments. Because phage material is required for many experiments, efficient propagation is essential. Previous data show that FLC6 and FLC4-4c propagation is not linearly proportional to available hosts. There seems to be an optimum where bacterial replication is maintained while the phages undergo multiple rounds of replication. Our model will attempt to predict this optimum based on experimental data.

Material & Methods

Bacterial propagation

Bacteria *Burkholderia glumae* strains (MAFF accession numbers 302552 and 302746) and *Burkholderia* plantarii strain (MAFF accession number 302909) were used. Both *B. glumae* and *B. plantarii* were cultured in potato-peptone-glucose (PPG) medium (2.5% (w/v) peptone, 2.5% (w/v) glucose, 1.5% (w/v) $Na_2HPO_4 \cdot 12H_2O$, and 0.25% (w/v) KH_2PO_4)(Sasaki et al., 2021). The potato infusion was made by boiling 20% (w/v) potatoes in water for 15 minutes. Either, 1.5% or 0.4% Agar was added to create the base and top agar respectively.

Ralstonia pseudosolanacearum strain (MAFF accession number 106603) was cultured in a casamino acid-peptone-glucose (CPG) medium (1.0% (w/v) peptone, 0.1% (w/v) casamino acids, and 0.5% (w/v) glucose) (Sasaki et al., 2021). The approximate CFU/ml based on OD_{600} values is 10^8 CFU/ml at an OD_{600} of 0.1 (Subedi et al., 2020; van der Wolf et al., 2022). The bacterial strains used in this project were provided by the NARO GeneBank (Tsukuba, Japan).

All strains were stored at -80°C and plated on 1.5% agar, at 28°C to isolate a single CFU. In preparation for experiments, an overnight culture with the respective liquid growth medium was made and placed in the shaking incubator (28°C, 200 rpm).

Phage propagation

Bacteriophages FLC4-4c, previously collected by (Sasaki et al., 2021), were amplified using *R. pseudosolanacearum* as a host. A dilution series of *R. pseudosolanacearum* was prepared in 2 ml LQ CPG, starting with an OD_{600} of 0.02 and ending at $0.02 \cdot 10^{-2}$, with a step size of $10^{-0.5}$. Approximately 5000 plaque-forming units (PFU) were added to these bacterial cultures. The cultures were placed in a shaking incubator at 28°C, 200 rpm, for 24 hours.

After the incubation period, the OD_{600} of each culture was measured. The dilution step showing the steepest drop in OD_{600} value was selected for further processing. The selected sample was centrifuged at 7000 rpm, 4°C for 5 min. The supernatant was collected and filtered using a 0.45 µm filter.

The PFU per microliter (PFU/µl) of the resulting phage stock was determined using a plaque assay. The remaining phage stock was stored at 4°C. To maintain high PFU/µl, the phage stock was generally replaced every month due to decreased viability over time.

Plaque assay

Plates with 1.5% CPG agar were preheated to 28°C. 0.5 ml liquid CPG containing 0.1 OD_{600} *R. pseudosolanacearum* was mixed with 5 ml (0.4%) 50 °C agar. The mixture was poured on the preheated plates and left to solidify. Thereafter, 10 µl droplets of serially diluted phage suspension were placed on top of the agar and left to dry. Upon drying the plates were placed in the incubator at 28 °C for 20 hours. The number of PFUs was recorded at the first dilution with limited plaque overlap. The plates were imaged and individual plaque size was estimated using ImageJ (version 1.54g).

Colony forming unit estimation

Bacterial cultures were grown overnight. The OD_{600} was taken and set to 0.2 in the appropriate media. A dilution series was made using the bacterial culture and sterilised demi-water. 10 µl droplets were plated on 1.5% agar plates and incubated at 28°C for 24 hours.

Bacterial growth assay

Over night cultures of *B. glumae, B. plantarii,* and *R. pseudosolanacearum* were set to an OD_{600} of 0.2 in 2 ml liquid media. The cultures were placed in the shaking incubator at 28°C, 200 rpm. Every hour, 100 µl was taken to measure the OD_{600}. The experiment was performed in duplo.

Binding efficiency assay

Bacteria were grown overnight and diluted with fresh medium 3 hours before the experiment to ensure they were in the exponential growth phase. Bacteria were diluted to an OD_{600} of 0.02 in 1 ml, in their appropriate media. FLC4-4c was added at a Multiplicity of Infection (MOI) of 1 and the solution was shaken before being placed in the shaking incubator at 28°C, 200 rpm, for the specified time. After incubation, the bacterial solution was centrifuged at 7000 rpm for 5 min at 4°C. 500 µl supernatant was carefully removed and used for the subsequent plaque assay (Khan Mirzaei & Nilsson, 2015).

Latency period and burst size

A homogenous *R. pseudosolanacearum* culture was picked from a single CFU and grown overnight in liquid CPG. Fresh CPG was inoculated with the ON culture to a set OD_{600} of 0.2 ($2 \cdot 10^8$ CFU/ml). Stock phage solution was added to achieve the desired MOI range (10, 5, 1, 0.5, 0.1 + Control). The cultures were placed at 28°C, 180 rpm. Every 30 min the cultures were observed for changes in turbidity. When free-floating particles were observed, the samples were spun down at 7000 rpm, 5 min, and 4°C and subsequently filtered using a 0.45 µm filter. The number of free-floating phages was measured using a plaque assay (Khan Mirzaei & Nilsson, 2015).

Mathematical model

Plate dynamics

The Plaque assay dynamics were simulated using Python version 3.8.10 64-bit | Qt 5.15.2 | PyQt5 5.15.10 | Windows 10 (AMD64). The scripts and parameters used in the presented simulations can be found on GitHub (https://github.com/MegaLeroy/Phage_Modelling_Internship). The script was based on the work by Chus Antoñanzas and heavily modified. The original code can be found at (https://github.com/chus-chus/cellular-automata/tree/master/experiment_templates). The general structure of the simulation is as follows. First, a two-dimensional square lattice for both the bacteria and the phages is generated with length *world size*. Each position in the bacterial lattice can be empty or inhabited by either healthy or infected cells. While the phage layer is filled with integers representing the number of phages present. The bacterial plane is filled according to the *bacterial density* (Figure 1 A). The phage plane is filled exclusively within a circle of *radius,* the number of phages added to the selected locations is equal to the *phage concentration* (Figure 1 C).

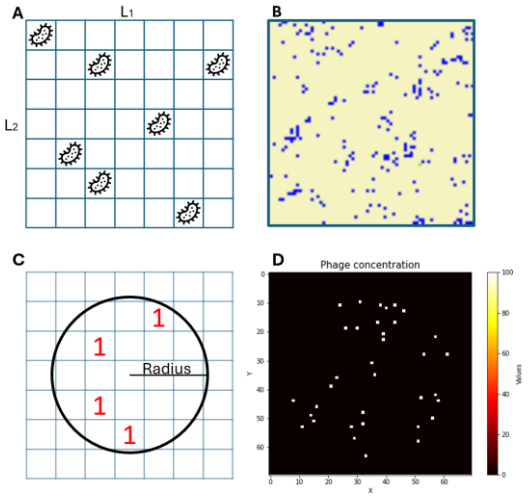

Figure 1, the Lattice structure of the model*. Schematic overview of the internal logic in the model (A & C), with the accompanying images created by the model (B & D). The placement of bacteria into the model is random and dependent on the bacterial density (A & B). The phage placement is restricted to a circular area in the center of the model. Again, phages are placed at random dependent on phage concentration (C & D).*

After initialisation, the lettice is iterated over a specified number of *epochs*. At each time step 6 main operations are performed: phage diffusion, bacterial replication, Infection, bacterial diffusion, lysis, and updating statistics. Phages can diffuse to their 8 neighbouring cells, being spread evenly between the available spaces.

Both infected and healthy bacteria replicate according to a set replication rate and the availability of nutrients. The rate of replication is linearly proportional to the percentage of nutrients available. Infection of Healthy bacteria happens depending on the infection rate (Ip), the number of phages in the corresponding phage plane position (P), and the percentage of nutrients available (N).

$$Infection\ propability = (1 - (1 - Ip)^{P}) * N$$

Bacterial diffusion occurs randomly according to the diffusion rate. If an empty neighbouring cell is available, bacteria have a chance of moving to the open space. Lysis is assumed to occur at an average rate of 1/*latent period*. With a standard Burst size (Bs) adding to the phage count when lysis occurs. Finally, for simplicity's sake, we utilise a single nutrient value which is distributed equally over the entire lattice. At the end of each time step, the unitless nutrient score is reduced by the number of bacteria present at that time step.

The two main limiting factors in the simulation are the time (*epochs*) and the *nutrient availability*. The latter is a *world size-dependent* constant which is reduced by the number of bacteria at each time step. After running the simulation an animation is created as well as a heat map of the phage plane and a record of variables.

Numerical cellular automata

Our numerical cellular automata utilised the same approach to simulating plate dynamics. Instead of any space being occupied by either no, healthy, or infected cells, this model allows for simultaneous occupation by multiple cells. Again, The created lattice has sides of length *world size*, with 3 layers to form a matrix. Layer one is filled with single bacteria during the initiation step according to the *bacterial density*. Layer 2 is initially empty, and is filled when bacteria from layer 1 are infected. The third layer represents the phages in the system and can again be filled according to a specified *phage density* and *radius*. For simplicity's sake, the nutrients are again assumed to diffuse at a rate high enough to use a single value for the entire plate. Previous models implemented multiple infections as a continuous factor, where infected cells could be further infected n times, absorbing more phage particles without increasing burst size (Cummings et al., 2012). For simplicity's sake, we restrict infection of cells to a single event. Still, multiple infections are possible and follow the Poisson distribution as described below.

Parameter motivation

After establishing the framework of the simulation, specific variables have to be obtained. This was done through the use of wet lab experiments (Table 1).

The relation between OD_{600} and bacterial density in *R. pseudosolanacearum* has been used previously. In literature, the assumption is that 0,1 OD_{600} *R. pseudosolanacearum* liquid culture contains between 1-2·10^8 CFU/ml (Álvarez et al., 2019; Caruso et al., 2002; van der Wolf et al., 2022). World size can be inferred from the plate size. Converting these measurements to the number of cells in the simulation was done by taking the smallest unit in the simulation (a bacterial cell). For *Burkholderia glumae,* they are rod-shaped with dimensions of 0.5–0.7 × 1.5–2.5 µm in width and length (HAM et al., 2010). Taking the average of these dimensions gives:

$$\sqrt{0.6 \cdot 2.0} = \sqrt{1.2\ \mu m^2} = 1.095\ \mu m$$

Dividing by this distance gives us the number of cells in each side of the lattice (Table 1). The bacterial replication rate was established using growth curves in liquid Cultures.

Table 1, Parameter values used in plate simulation.

Parameter	Value
Bacterial density	9.43·10^{-3}CFU·cell^{-1}
World size • Plate • Droplet • Single PFU	 90mm: 99666 cells 12mm: 13288 cells 1mm: 1107 cells
Bacterial replication rate	0.0416 min^{-1}
Bacterial diffusion	Arbitrary
Latency period	180 min
Burst size	200
Infection rate	1
Phage diffusion rate	Arbitrary
Nutrient density	Time-dependent
Carrying capacity	9.34 CFU·pixel^{-1}

Poisson distribution

The estimated number of phage infections per bacteria was calculated and visualized using Python. The input required the MOI, infectivity, and the number of time steps. The standard Poisson probability function was used where P(k) is the probability a cell will be infected with k phages. Λ is the adjusted MOI, here low infection rates decrease the MOI and extended time steps increase it.

$$P(\ ) = \frac{\lambda^k e^{-\lambda}}{k!}$$

Results

Burkholderia plantarii shows consistent abrupt disappearance in plaque formation

When creating the model, the central question was; what characteristics cause the abrupt disappearance of plaque-forming units in *Burkholderia plantarii* cultures? This effect was verified by performing a plaque assay with the same FLC4-4c phage on *R. pseudosolanacearum, B. glumae* and *B. plantarii* bacterial lawns (Figure 2). As expected, the plaques formed on *R. pseudosolanacearum* and *B. glumae* followed the gradual decline in PFU's count. There was a difference in the final plaque formation based on specific susceptibility to the phage between the two hosts. In the *B. plantarii* sample, complete clearance was observed in the 10^{-2} dilution. Based on the PFU count on *R. pseudosolanacearum* there would be about 6800 phages present at the 10^{-2} dilution. One dilution later we would expect to see 680 phages, but 0 PFUs can be found (Figure 2).

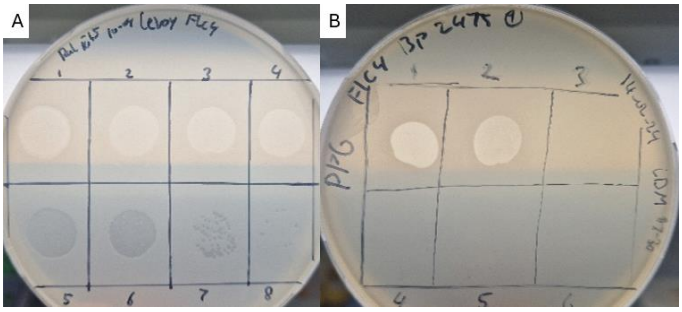

Figure 2, Plaque assays on R. pseudosolanacearum and B. plantarii. *Plaque assays with the same FLC4-4c strain were performed on both R. pseudosolanacearum (A) and B. plantarii (B). The Image was taken 24 hours after plating and shows the dilution series from 10^{-1} to 10^{-8} indicated by the number next to the square.*

Colony forming units

The main method for assessing bacterial concentrations is measuring the Optical density$_{600}$ (OD_{600}). To connect the OD_{600} to the number of bacteria in a solution, we performed multiple CFU assays for *R. pseudosolanacearum*. The shown dilution series was conducted in triplet, giving an average CFU/ml of $1.85 \cdot 10^8$. This value was close to those found in the literature and will be used to calculate the MOI and number of bacteria in the models from here on out.

The burst size and latent period

The burst size and latent period are useful phage-specific parameters that allow for more accurate predictions of phage population dynamics. Here we estimate the latent period by observing changes in turbidity for phage-treated samples. A drop in LQ turbidity is associated with the Lysis of bacterial cells. Upon observing this drop, the samples were filtered to avoid further infection and used in a plaque assay. *R. pseudosolanacearum* infected with FLC4-c4 showed changes in turbidity after 180 min of incubation (Table 2). The change translates poorly to OD_{600} measurements as the conjugated debris of lysed cells clumps together. At 180 min, the control sample showed a homogenous mist when shaken, while the 10 and 5 MOI showed larger string-like clumps with the rest of the culture appearing less clouded. The 1, 0.5, and 0.1 MOI samples showed some drop in turbidity, but not to the same extent as in the higher MOI samples. The limited Lysis observed in the 1 MOI sample can be explained by the Poisson distribution, which predicts only 63% of bacteria will be infected (Figure 3). Meanwhile, at an MOI of 10 or 5, approximately 100% and 99% of bacteria are expected to be infected, respectively.

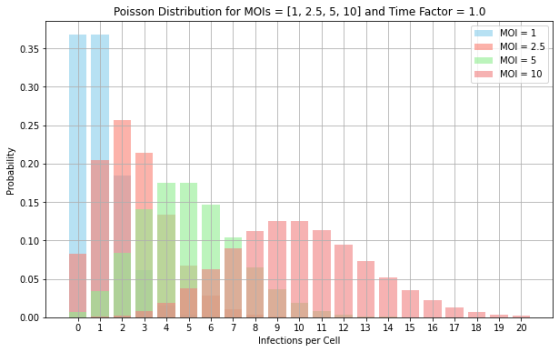

Figure 3, Prediction of number of infections per bacteria given a specific MOI. *The percentage-wise distribution of infection quantities is given for several MOI values. The y-axis describes the percentage of infections, and the x-axis gives the number of phages that are predicted to bind to a single bacterium.*

Upon observing a drop in turbidity of the liquid culture, which indicates successful lysis, the samples were filtered and plated. The latent period and the calculated burst size can be found in Table 2.

Table 2, Phage burst size and latent period for three bacterial strains at a multiplicity of infection (MOI) of 5 or 10.

Strain	**Latent period (min)**	**PFU/µl**	**Burst size**
R. pseudosolanacearum (MOI 5)	180	$4.0 \cdot 10^7$	200
R. pseudosolanacearum (MOI 10)	180	$4.1 \cdot 10^7$	205
B. glumae (MOI 5)	150	$7 \cdot 10^4$	0.35
B. glumae (MOI 10)	150	$1.9 \cdot 10^5$	0.95
B. plantarii (MOI 5)	150	$1.5 \cdot 10^5$	0.75
B. plantarii (MOI 10)	150	$2.2 \cdot 10^5$	1.1

The latent period between the hosts was comparable, with clear lysis being observed around the 150 to 180-minute range. While the latent period is similar, the burst size is vastly different. *R. pseudosolanacearum* shows a burst size of 200, which is larger than expected for a jumbo phage. While both *B. plantarii* and B. glumae show burst sizes below minimum replication.

Binding efficiency and respective MOI experiment

Binding efficiency of FLC4-4c on several hosts was tested. Upon combining phages with the bacteria, they were mixed thoroughly and then placed in the centrifuge to separate bound and unbound phages. The MOI used was 1 and the time for binding of 3 or 10 minutes. The resulting CFUs are shown in Table 3.

Table 3, Binding efficiency results. The number of unbound FLC4-4c jumbo phages is given after 3 and 10 minutes for three bacterial strains.

Strain	Time	PFU/µl
R. pseudosolanacearum	3 min	$2.9 \cdot 10^4$
	10 min	$2.3 \cdot 10^4$
B. glumae	3 min	$3.4 \cdot 10^4$
	10 min	$2.3 \cdot 10^4$
B. plantarii	3 min	$3.4 \cdot 10^4$
	10 min	$2.2 \cdot 10^4$
Control	X	$2.9 \cdot 10^4$

There is a clear decrease in free-floating phages between the samples at 3 and 10 minutes. However, the control which was derived from liquid culture mixed with the phage solution, shows fewer free-floating phages than the 3 min samples. In theory, the control should give the highest phage count in the plaque assay, as no phages would be absorbed in the treatment.

Computational analysis

Plaque size analysis

Several plaque assays were performed during the project and images were taken for recordkeeping. Additionally, these images were used to calculate the plaque size for each distinguishable plaque at a given dilution. The range of plaque sizes was compiled and compared to the model's observed plaque sizes (Figure 5).

Comparing model with reality

The cellular automata representing bacterial growth on plates was established by recreating known functions and fitting the parameters with experimentally acquired data. Before diving into possible mechanisms behind the abrupt decline in PFU formation in *B. plantarii*, we inspected the model's behaviour for *R. pseudosolanacearum* growth. Using the parameters as described in Table 1, we can show plaque formation after 24 hours on a plate. The growth of the bacterial carpet and the formation of the plaque seem to follow in vitro experiments. An interesting phenomenon observed in the simulation is a variation in plaque size. At first, this was thought to be an artifact of the simulation. Upon further exploration, it was found that the distribution in the simulation closely follows those observed in wet-lab experiments (Figure 4). While the relative size of the plaques is following reality, the absolute size is observed to be smaller than expected. Since 1 pixel in the simulation represents 1.2 µm^2, the average simulated diameter is 72.6 µm. In wet-lab data, this is found to be 424 µm.

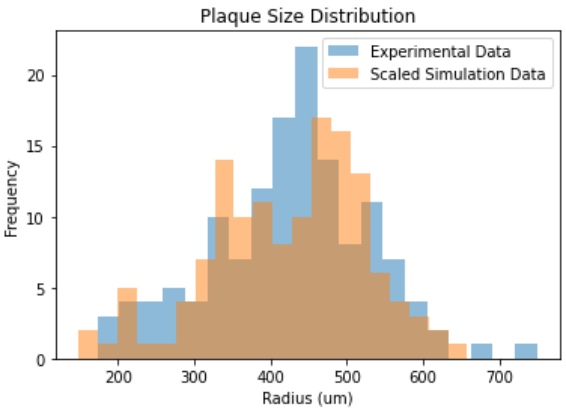

Figure 4, Histogram comparing plaque size on a plate and in categorical simulation. *Plaque radia were measured based on their total area. The radius of the simulated samples was automatically calculated. Each simulated data point was shifted to have the same mean as the experimental samples. Experimental Mean: 424.48 µm, Std: 104.79 µm. Scaled Simulation Mean: 424.48 µm, Std: 102.08 µm.*

Meanwhile, the second model created which clusters multiple cells together to increase the observable density in an area shows the following distribution (Figure 5). Here the standard deviation is much lower at 15,70. Even when adjusting for the new pixel-to-distance ratio, the standard deviation is still only 47.1 µm.

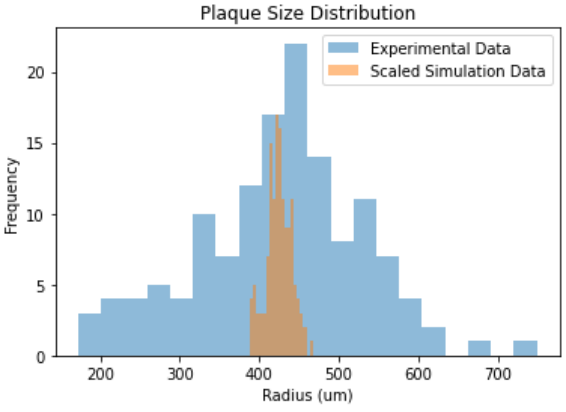

Figure 5, Comparing plaque size on plate and in numerical simulation. *Plaque radia were measured based on their total area.*

The radius of the simulated samples was automatically calculated. Each simulated data point was shifted to have the same mean as the experimental samples. Experimental Mean: 424.48 µm, Std: 104.79 µm. Scaled Numerical Simulation Mean: 424.48 µm, Std: 15.70 µm.

Density-dependent resistant bacteria show the same gradual decline in the simulation

Bacterial density was calculated as a percentage of the carrying capacity of bacteria.

$$Bacteria\ density = \frac{Bacterial\ number}{Carrying\ capacity}$$

The Bacterial density could then be to regulate the infection rate of phages. The progression of resistance was set to follow one of three formulas. The first, y = 1 - x^3, provides low resistance at lower densities (Sup Figure 1). At higher densities, the level of resistance increases greatly. The bacterial density at which 50% resistance is reached was 0.79 (Sup Figure 1). When using this density-dependent resistance and slowly lowering the phage concentration, we were not able to show the abrupt disappearance of plaques (Figure 6). The second ($(1-x)^2$) and third (e^{-5x}) formulas were much steeper in their resistance progression (Sup Figure 1). These had a respective halfway point of 0.29 and 0.14. The additional resistance did result in slightly smaller plaques, but no overall abrupt decline in plaque formation was shown.

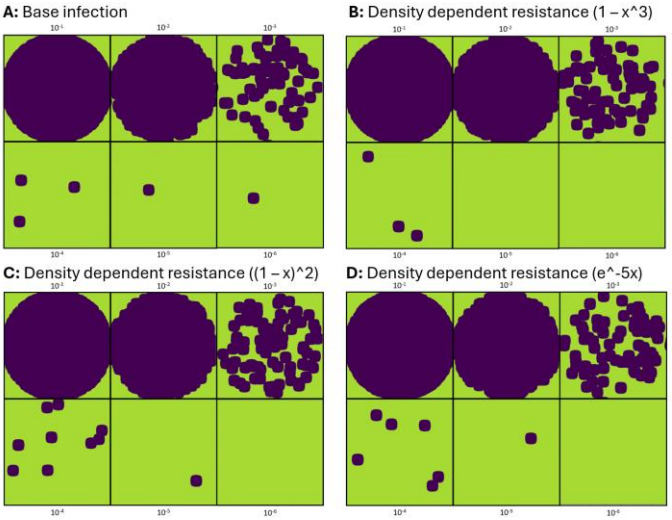

Figure 6, Collection of plaque assay simulations with varying density-dependent resistances. *Each panel shows a simulation of 1 decreeing phage concentration. Starting at a concertation of around 6800 and decreasing by steps of 10. The green space is filled with bacteria and the plaques are in blue. (A) base model with no added density-dependent resistance. (B-D) formulas to describe the degree of resistance were used: y = 1 - x3 (B), $(1-x)^2$ (C), e^{-5x} (D).*

Discussion & Conclusion

The goal of this project was to better understand plaque formation in *Burkholderia plantarii* and its abrupt disappearance. Our strategy combined wet-lab experiments with computational modelling to create a model that could predict the abrupt disappearance of successful phage infections based on local bacterial densities. First, we recreated the previously observed phenomenon in multiple *B. plantarii* strains (MAFF accession numbers 302475, 302909, and 3017237). Thereafter a model was created to recreate the gradual plaque formation as observed in *Ralstonia pseudosolanacearum* bacterial lawns. Despite following the growth and distribution of plaque formation quite closely as observed in *R. pseudosolanacearum,* we were unable to recreate the abrupt disappearance as observed in *B. plantarii*. Even with the implementation of density-dependent resistance, the development of successful infections happened so early in the simulation that the special separation of the phages did not allow for sufficient interaction between infection sites.

Verification of the previously observed abrupt vs Gradual decline in plaque formation in several FLC4-4c hosts

While confirming the previously observed phenomenon of abrupt PFU reduction, we found each of the *B. plantarii* strains used showed the expected result. Indicating the mechanisms behind the effect is somewhat conserved within the species. Note that in preliminary data on multi-generational adaptation to *B. plantarii* has shown the effect can be broken. When selectively growing FLC4-4c on *B. plantarii* for multiple generations the gradual reduction in PFUs within the dilution series returns. Additionally, after multiple generations, it appears that the infection rate increases on the selected host, while other hosts become less viable for the selected phages.

Model Bacterial concentration as compared to optical density measurements

The confirmation of bacterial density was used to confirm the multiplicity of infection numbers used in several experiments. This was to ensure infection coverage over the bacterial population used was sufficient. Additionally, the bacterial concentration was used for modelling purposes. Both in the establishment of initial bacterial concentrations over the lattice as well as the expected carrying capacity of the selected medium. The average bacterial concentration found for *R. pseudosolanacearum* was 9.25 * 10^8 CFU/ml/OD, which closely resembles the 10^9 CFU/ml/OD found in the literature (Subedi et al., 2020; van der Wolf et al., 2022). The highest OD_{600} measurements for completely overgrown *R. pseudosolanacearum* cultures was around OD_{600} of 10. While high, this means each bacteria had

100 μm^3 to itself or a box with sides of 4.64 µm around it.

Burst size and latent period estimations of *R. pseudosolanacearum, B. plantarii,* and *B. glumae*

Previous research has highlighted the effects variability in burst size, latent period, and eclipse time have on plaque size (Abedon et al., 2003; Abedon & Culler, 2007b). The parameter values were established in *R. pseudosolanacearum* but proved more difficult in to estimate in *B. plantarii* and *B. glumae*. The main method used in the literature was to repeatedly measure the OD_{600} value of liquid cultures to establish when lysis occurs. However, in our results even in successful amplification of FLC4-4c the OD_{600} value of the solution kept increasing over time. The ultimate OD_{600} value was lower in efficiently lysated samples compared to those with higher bacterial concentrations at the start. Therefore, repeatedly measuring the OD_{600} was much more prone to recording measurement errors instead of indicating when lysis occurred. We did find that at a certain time after combining the bacteria and phages an accumulation of debris would occur in the solution. This was thought to be the clustering of proteins and membrane components from successfully lysated samples, but this was not confirmed. The presence of this debris in the higher MOI (5 & 10) and the apparent absence in the control made us confident it was, in fact, an indication of successful lysis. Therefore, we observed the samples over time and filtered them once the debris was clearly visible.

To ensure complete lysis of the host bacteria, we utilized MOIs of 0, 1, 5, and 10. Following the Poisson distribution (Figure 5) we can see that an estimated 0%, 63%, 99%, and 100% of hosts would have at least one infecting phage respectably. Combined, this results in the apparent complete lysis of *R. pseudosolanacearum* after 180 minutes, which is slightly faster than the 270 minutes observed in *Ralstionia* infecting RsoM2USA (Ahmad et al., 2021). Despite the shorter latency period, the observed burst size of 200 was significantly higher than the 32 observed RsoM2USA. 2 more jumbo phage that infect *Ralstonia*, ϕRSF1 & ϕRSL2, with a latency period of 150 min and burst size of 75 and 40-50 respectively (Bhunchoth et al., 2016).

The measurements for *B. plantarii* and *B. glumae* were more difficult to interpret. The conflicting observations stem from the fact that the debris generation did follow that of the *R. pseudosolanacearum* samples where accumulation was first observed at 150 min in the higher MOI samples, but not in the control (and to some extent in the MOI 1 sample). Despite the apparent successful lysis of the host, subsequent plaque assays showed an average burst size of around 1. This was in the same order of magnitude as the initial phage concentration. Multiple explanations for the observations are possible. Starting with the discrepancy in infection efficiency. The previously presented MOI ratios mentioned earlier were based on the assumption of close to 100% infection efficiency. However, looking at a plaque assay with the sample FLC4-4c1 Jumbo phage on different hosts shows the PFU numbers are much lower in both *B. plantarii* and *B. glumae*. This reduced "real" MOI can explain why estimation in *B. plantarii* was not successful. However, looking at *B. glumae* compared to *R. pseudosolanacearum* we find a reduction in PFU of about 20. Therefore, directly translating this to infection efficiency would give an efficiency of 5%. Recalculating the MOI with this efficiency still predicts that the MOI 10 sample would result in 39% hosts with at least one successful infection (Figure 3). Therefore, the observed burst size of 1 can still not be explained.

Binding efficiency is lower than expected

The results of our binding experiment were difficult to interpret due to unexpected plaque formation in the control. In these experiments we did not use protein-coated Eppendorf tubes, possibly resulting in phage particles binding to the tube walls. To confirm the results this oversight should be corrected. Despite this, we can observe an absorption of about 32% after 10 minutes (If the 3-minute measurement is assumed to represent 100% unbound phages). This binding efficiency is much lower than that found in non-jumbo phages such as *Escherichia coli* infecting phages with absorption rates between 90-98% after 5 minutes (Khan Mirzaei & Nilsson, 2015). When comparing to another jumbo phage vB_OspP_OH, they find similar absorption rates of 30% after 10 minutes (Decewicz et al., 2020). One aspect we speculated and Decewics *et al*., showed that increased bacterial concentrations correlate with higher absorption rates of 70% (0.2 OD) and 80% (0.4 OD). Considering our used OD was 0.02 which correlates to an average volume of $5 * 10^4$ μm^3 per bacteria, we expect increasing the bacterial concentration will significantly increase the likelihood of a phage being absorbed by a bacterium.

Modelling of plaque formation fails to recreate the abrupt disappearance of plaques.

The created model was compared to reality based on the variation of created plaques. Images from wet lab experiments were compared to simulated single plaques. The resulting size distribution was compared in Figure 4. The original categorical simulation showed a highly similar size distribution compared to the one found in experiments. Our second iteration of the model fails to follow the same distribution and has a much smaller standard deviation. We believe the difference in models and their size distribution stems from the inherent randomness in the first model. Where movement and replication occurred randomly. This combined with the on or off state of infection in the bacteria made the spread of the infection highly variable. Despite the retainment of random placement of starting bacteria in the second model, we see a severe reduction in plaque size variation. Here the replication of bacteria is based on the current bacterial concentration. Additionally, the spread of bacteria is only initiated when each of the surrounding cells can receive an equal number of bacteria, further reducing random spread in the system. Despite the apparent departure from the biological example, we believed the reduced randomness would not hinder the mechanism behind the abrupt disappearance of plaques.

None of the density-dependent resistance factors reproduced the abrupt disappearance in plaque formation.

The main factor that changes between the different dilutions is the number of phages and therefore the ratio between phage and bacteria. As we found previously the original position of phages and therefore the average time it takes for bacteria to spear and make contact with them changes. We decided to focus on density-dependent resistance as a possible explanation for the abrupt disappearance of plaque formation. Using several different equations each with their own resistance progression we were unable to recreate the observed effect. Even the most resistant variant, where only filling 14% of the carrying capacity results in 50% resistance, did not observe a significant reduction in the created plaques.

It turns out that the observed cut-off points between a phage count of 6800 to 680 represent an MOI difference of 0.01 to 0.001 Meaning individual success of phage infection is dependent on phage presence 107 to 339 µm away on average. Within our model, the local bacterial concentration and infection progress at this range are not taken into account. One could consider creating a global value which does follow such values. However, the assumption that signalling molecules can be produced and distributed at those speeds seems improbable.

References

Abedon, S. T., & Culler, R. R. (2007a). Bacteriophage evolution given spatial constraint. *Journal of Theoretical Biology*, *248*(1), 111–119. https://doi.org/10.1016/j.jtbi.2007.02.014

Abedon, S. T., & Culler, R. R. (2007b). Optimizing bacteriophage plaque fecundity. *Journal of Theoretical Biology*, *249*(3), 582–592. https://doi.org/10.1016/j.jtbi.2007.08.006

Abedon, S. T., Hyman, P., & Thomas, C. (2003). Experimental Examination of Bacteriophage Latent-Period Evolution as a Response to Bacterial Availability. *Applied and Environmental Microbiology*, *69*(12), 7499–7506. https://doi.org/10.1128/AEM.69.12.7499-7506.2003

Adachi, N., Tsukamoto, S., Inoue, Y., & Azegami, K. (2012). Control of Bacterial Seedling Rot and Seedling Blight of Rice by Bacteriophage. *Plant Disease*, *96*(7), 1033–1036. https://doi.org/10.1094/PDIS-03-11-0232-RE

Ahmad, A., Addy, H., & Huang, Q. (2021). Biological and Molecular Characterization of a Jumbo Bacteriophage Infecting Plant Pathogenic Ralstonia solanacearum Species Complex Strains. *Frontiers in Microbiology*, *12*, null. https://doi.org/10.3389/fmicb.2021.741600

Álvarez, B., López, M., & Biosca, E. (2019). Biocontrol of the Major Plant Pathogen Ralstonia solanacearum in Irrigation Water and Host Plants by Novel Waterborne Lytic Bacteriophages. *Frontiers in Microbiology*, *10*, null. https://doi.org/10.3389/fmicb.2019.02813

Bhunchoth, A., Blanc-Mathieu, R., Mihara, T., Nishimura, Y., Askora, A., Phironrit, N., Leksomboon, C., Chatchawankanphanich, O., Kawasaki, T., Nakano, M., Fujie, M., Ogata, H., & Yamada, T. (2016). Two asian jumbo phages, ϕRSL2 and ϕRSF1, infect Ralstonia solanacearum and show common features of ϕKZ-related phages. *Virology*, *494*, 56–66. https://doi.org/10.1016/j.virol.2016.03.028

Caruso, P., Gorris, M. T., Cambra, M., Palomo, J. L., Collar, J., & López, M. M. (2002). Enrichment Double-Antibody Sandwich Indirect Enzyme-Linked Immunosorbent Assay That Uses a Specific Monoclonal Antibody for Sensitive Detection of Ralstonia solanacearum in Asymptomatic

Potato Tubers. *Applied and Environmental Microbiology*, *68*(7), 3634–3638. https://doi.org/10.1128/AEM.68.7.3634-3638.2002

Cummings, K. W., Levy, D. N., & Wodarz, D. (2012). Increased burst size in multiply infected cells can alter basic virus dynamics. *Biology Direct*, *7*(1), 16. https://doi.org/10.1186/1745-6150-7-16

Decewicz, P., Golec, P., Szymczak, M., Radlinska, M., & Dziewit, L. (2020). Identification and Characterization of the First Virulent Phages, Including a Novel Jumbo Virus, Infecting Ochrobactrum spp. *International Journal of Molecular Sciences*, *21*(6), Article 6. https://doi.org/10.3390/ijms21062096

Gallet, R., Kannoly, S., & Wang, I.-N. (2011). Effects of bacteriophage traits on plaque formation. *BMC Microbiology*, *11*(1), 181. https://doi.org/10.1186/1471-2180-11-181

HAM, J. H., MELANSON, R. A., & RUSH, M. C. (2010). Burkholderia glumae: Next major pathogen of rice? *Molecular Plant Pathology*, *12*(4), 329–339. https://doi.org/10.1111/j.1364-3703.2010.00676.x

Kanaizuka, A., Sasaki, R., Miyashita, S., Ando, S., Ito, K., Fukuhara, T., & Takahashi, H. (2023). Isolation of Burkholderia jumbo phages and their utilization as biocontrol agents to suppress rice seedling rot disease. *Journal of General Plant Pathology*, *89*(1), 24–34. https://doi.org/10.1007/s10327-022-01107-z

Khan Mirzaei, M., & Nilsson, A. S. (2015). Isolation of Phages for Phage Therapy: A Comparison of Spot Tests and Efficiency of Plating Analyses for Determination of Host Range and Efficacy. *PLOS ONE*, *10*(3), e0118557. https://doi.org/10.1371/journal.pone.0118557

Sasaki, R., Miyashita, S., Ando, S., Ito, K., Fukuhara, T., & Takahashi, H. (2021). Isolation and Characterization of a Novel Jumbo Phage from Leaf Litter Compost and Its Suppressive Effect on Rice Seedling Rot Diseases. *Viruses*, *13*(4), Article 4. https://doi.org/10.3390/v13040591

Subedi, N., Taylor, C. G., Paul, P. A., & Miller, S. A. (2020). Combining partial host resistance with bacterial biocontrol agents improves outcomes for tomatoes infected with *Ralstonia pseudosolanacearum*. *Crop Protection*, *135*, 104776. https://doi.org/10.1016/j.cropro.2019.03.024

van der Wolf, J., Kastelein, P., Poleij, L., Krijger, M., Mendes, O., Sedighian, N., Allen, C., Bonants, P., & Kurm, V. (2022). Factors influencing Ralstonia pseudosolanacearum infection incidence and disease development in rose plants. *Plant Pathology*, *71*(7), 1619–1632. https://doi.org/10.1111/ppa.13596

Use of language model

This report has utilised a machine-learning language generation model (ChatGTP-3.5) intending to improve readability. The use was limited to spelling checks, grammatical suggestions and paragraph organisation. The main author has reviewed and revised every section to ensure accuracy and clarity.

Supplemental data

Sup Table 1, Host range of bacteriophage FLC6 as presented by (Sasaki et al., 2021)

Species	Strain	Sensitivity [2]
B. glumae	MAFF106619	+
B. glumae	MAFF301169 [1]	+
B. glumae	MAFF302417	+
B. glumae	MAFF302552	+
B. glumae	MAFF302746	+
B. plantarii	MAFF106727	+
B. plantarii	MAFF302466	+
B. plantarii	MAFF302475	+
B. plantarii	MAFF302909	+
B. plantarii	MAFF302912	+
B. plantarii	MAFF302936	+
R. pseudosolanacearum	MAFF106603	+
R. pseudosolanacearum	MAFF106611	+
R. pseudosolanacearum	MAFF211270	–
R. pseudosolanacearum	MAFF301485	–
R. syzygii subsp. indonesiensis	MAFF211271	–
R. syzygii subsp. indonesiensis	MAFF327032	–

Calculations

Plate size 90 mm, starting OD 0.1 in 0.5 ml, max OD 10 in 5.5 ml, clustered 9 *1.2 um^2 pixels

$$90\,mm = 90\,000\,\mu m$$
$$\pi * 45\,000^2 \mu m = 6.36 * 10^9 \mu m^2$$
$$0.5\,ml * 0.1\,OD * 10^9\,{}^{CFU}/_{ml * OD} \,/6.36 * 10^9 \mu m^2 * 10.8\,{}^{\mu m^2}/_{Pixel} = 8.4910^{-2}\,{}^{CFU}/_{pixel}$$

Carrying capacity:

$$5.5\,ml * 10\,OD * 10^9\,{}^{CFU}/_{ml * OD} \,/6.36 * 10^9 \mu m^2 * 10.8\,{}^{\mu m^2}/_{Pixel} = 93.4\,{}^{CFU}/_{pixel}$$

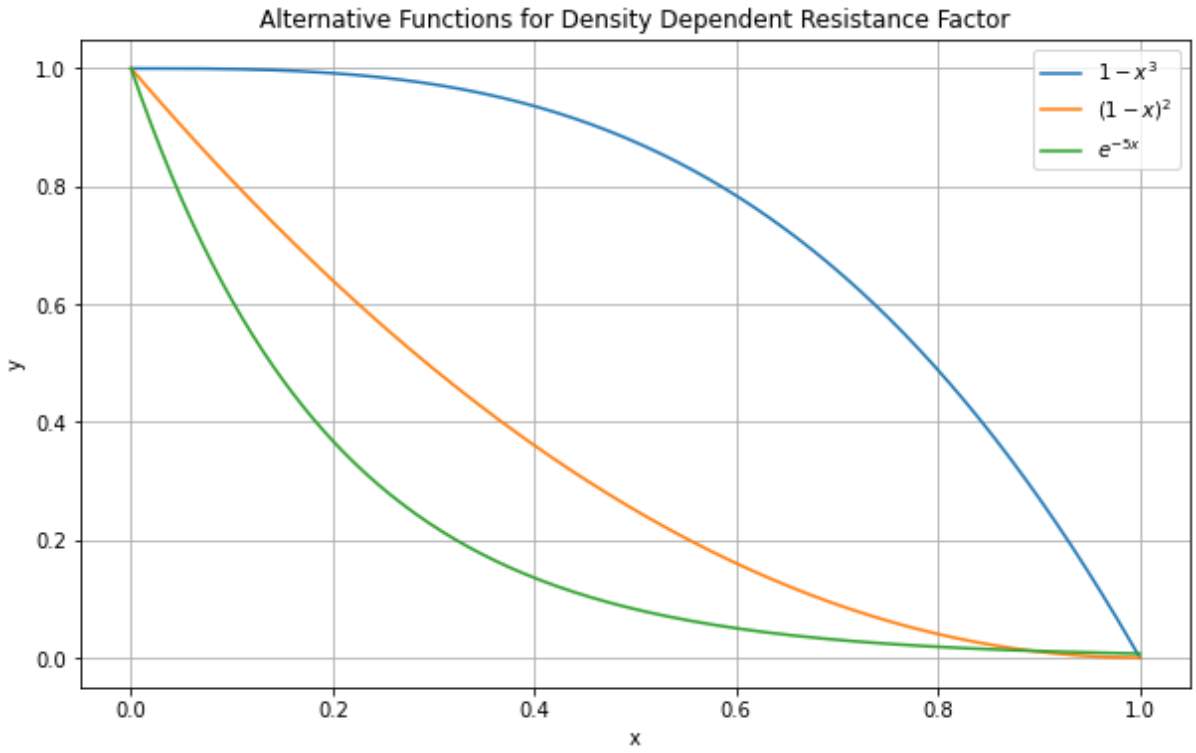

Sup Figure 1, Plot of density-dependent resistance formulas. The graph shows the bacterial concentration as compared to the carrying capacity on the x-axis. And the successful infection rate on the y-axis. The lines follow different formulas y = 1 - x^3 (Blue), $(1-x)^2$ (Orange), and (e^{-5x}) (Green).

Sup Table 2. Previously acquired plaque assay results

Observations at 48 hrs						
Neriza's FLC4-4c1 samples						
Bacteria	**Dilution**					
	-1	**-2**	**-3**	**-4**	**-5**	**-6**
***B. glumae* (302552)**	*	*	#	+	11	0
***B. glumae* (302746)**	*	*	*	*	59	5
***B. plantarii* (302909)**	*	*	0	0	0	0
***Ralstonia* (106603)**	*	*	*	57	4	0
Shuhei's FLC4-4c1 samples						
Bacteria	**Dilution**					
	-1	**-2**	**-3**	**-4**	**-5**	**-6**
***B. glumae* (302552)**	*	*	62	13	0	0
***B. glumae* (302746)**	*	*	*	74	15	2
***B. plantarii* (302909)**	*	*	0	0	0	0
***Ralstonia* (106603)**	*	*	*	68	7	0